Modeling the polydomain-monodomain transition of liquid crystal elastomers

Jonathan K. Whitmer, Tyler F. Roberts, Raj Shekhar, Nicholas L. Abbott, and Juan J. de Pablo

Modeling the Polydomain–Monodomain transition of Liquid Crystal Elastomers

Jonathan K. Whitmer,[1] Tyler F. Roberts,[1] Raj Shekhar,[1] Nicholas L. Abbott,[1] and Juan J. de Pablo[2, *]

[1]*Department of Chemical and Biological Engineering,*
University of Wisconsin, Madison WI 53706-1691
[2]*Institute for Molecular Engineering,University of Chicago, Chicago, IL 60637*

We study the mechanism of the polydomain–monodomain transition in liquid crystalline elastomers at the molecular scale. A coarse-grained model is proposed in which mesogens are described as ellipsoidal particles. Molecular dynamics simulations are used to examine the transition from a polydomain state to a monodomain state in the presence of uniaxial strain. Our model demonstrates soft elasticity, similar to that exhibited by side-chain elastomers in the literature. By analysing the growth dynamics of nematic domains during uniaxial extension, we provide direct evidence that at a molecular level the polydomain–monodomain transition proceeds through cluster rotation and domain growth.

Liquid crystalline elastomers (LCEs) combine the elastic properties of conventional rubbers with the optical properties of liquid crystals (LCs) [1]. This coupling gives rise to unusual physical properties [2–4] that have enabled a wide spectrum of applications, ranging from actuators [5], to artificial muscles [6] and optical-band materials [7]. Nematogens in LCEs are either crosslinked to an elastomeric network, resulting in side-chain LCEs (SCLCEs), or they are actually part of the network, resulting in main chain LCEs [1]. Both forms often exhibit a polydomain structure in the nematic and smectic states [8, 9], characterized by large, independently oriented domains. The absence of a global director renders these materials opaque. Upon application of sufficiently large uniaxial stress, however, LCEs undergo a polydomain-to-monodomain (P–M) transition [10, 11] whereby the domains align, resulting in a transparent material. After an initial elastic restoring force is overcome, the stress–strain curve exhibits a distinct plateau, where a small change to the applied stress induces a large deformation of the sample. Such a feature is often indicative of an underlying phase transition. In the general area of LCEs, this behavior is known as soft elasticity [1, 12, 13]. Upon reaching the monodomain state, traditional elastic response is restored.

The plateau stress σ_c is related to by the polymer backbone anisotropy ratio, $\ell_\parallel/\ell_\perp$, through the relation

$$\sigma_c = \mu \left(\ell_\parallel/\ell_\perp - 1 \right) , \qquad (1)$$

where μ is the bulk rubber modulus [14]. The anisotropy ratio quantifies the polymer radius of gyration parallel ($\ell_\parallel$) and perpendicular ($\ell_\perp$) to the local nematic director [1]. Main-chain LCEs tend to have large anisotropy ratios due to incorporation of rigid nematogens in the polymer backbone, giving rise to large plateau stresses. Conversely, side-chain LCEs yield more easily. As the anisotropy ratio approaches unity, the critical stress for the onset of soft elasticity disappears [14]. Experimental studies of LCEs show that the stress–strain plateau is strain-rate dependent. The quasi-static or equilibrium behavior exhibits no initial elastic regime, transitioning

directly from semi-soft to elastic response when domains align [15].

Several intriguing applications for LCEs, including their use as artificial muscles [6], rely on an underlying P–M transition. It has been proposed that this transition occurs due to domain reorientation toward the direction of applied stress, rather than by domain growth [16, 17]. This proposition has emerged from a combination of optical microscopy, X-ray scattering, and polarized light scattering measurements [18]. However, essential details remain unexplained, including the molecular origins of polydomain transformation, the effect of strain on size and orientational distribution of domains, and how individual domains respond to the application of strain. Understanding these details could enable design of LCEs with dynamic and mechanical responses tailored for specific applications.

Theoretical studies of LCEs have been performed at the continuum level based on anisotropic rubber elasticity theory [1]. Fridrikh and Terentjev [14] attributed the polydomain state of LCEs to quenched orientational disorder. In their model, crosslinks are not free to rotate and impart a quenched direction to the material, giving rise to the polydomain state through a coupling to the surrounding mesogens. Their model has served to rationalize a number of experimental observations at the level of nematic domains. However, in order to understand the underlying mechanism involved in the P–M transition, it is of interest to examine the system at the molecular scale.

Domain-level studies of LCEs have relied on lattice models and mean-field theory [19] or Monte-Carlo simulations [20, 21]. Off-lattice simulations of main-chain [22] and side-chain [23] elastomers have also been performed, but such studies where focused on the isotropic–nematic transition, and did not resolve the P–M transition. More specifically, there are no reports on the P–M transition on the basis of detailed many-particle models. In this work we therefore begin by proposing a molecular model that exhibits a polydomain state. The model is based on a representation of LC molecules as ellipsoidal parti-
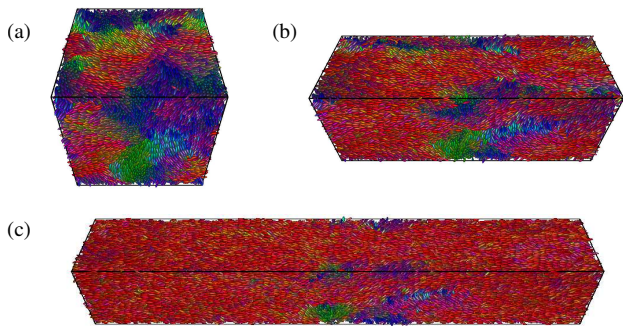
FIG. 1. (Color Online) Representative configuration of LCEs with rigid crosslinkers at various points of a constant strain-rate simulation with $N = 77824$ particles. Each particle is assigned an rgb (grayscale) value (x, y, z) equal to their orientation vector $\mathbf{n}$. (a) Initial configuration, showing a clear polydomain structure. The average domain size is $\langle N \rangle \approx 150$ particles, with 11 clusters having more than one thousand particles. (b) Under a strain $\varepsilon = 1.0$, domains begin to align and join. (c) At strain $\varepsilon = 2.5$, only small misaligned clusters remain. The global order parameter for the latter system is $S = 0.78$.

cles [24, 25]. Experimentally, crosslinking molecules in an elastomeric network may be either flexible or rigid [26]. Rigid crosslinkers enhance the anisotropy in the LCE and provide stability to the elastomeric network. Our model consists of a SCLCE with rigid crosslinkers, whose interactions have been tuned to promote local ordering to the easy axis of the crosslinker. We find that this model does exhibit a polydomain to monodomain transition, and we show that such a transition occurs through the reorientation of individual domains whose size and orientational distribution are functions of applied strain.

An atomic-level representation of LCEs is beyond the reach of current computational resources. Previous quasi-atomic level descriptions using bead-spring polymers and rods were limited to ≈ 2400 mesogens [23]. System sizes must be increased considerably if one is to capture the P–M transition, thereby necessitating further coarse-graining. In experiment, LC molecules are connected with flexible spacers to form backbone polymer chains. These polymer chains are then crosslinked to form the elastomeric network of LCEs. We represent these rigid crosslinking molecules as ellipsoids of the same size and shape as the model mesogens. Flexible spacers between LC molecules are described by fluctuating bonds whose length is based on the distance between the centers of mass of the LC molecules. Note that this representation allows the mesogens to rotate freely relative to the elastomeric network, subject to the steric hindrance of other particles. We therefore expect the anisotropy ratio to approach unity ($\ell_\parallel / \ell_\perp \approx 1$).

The ideal elastomeric network considered in this Rapid Communication consists of tetra-functional crosslinks and a perfect diamond network topology [27] in order to avoid introducing directional bias. The network is entanglement-free, with four or eight unit cells in all three orthogonal directions. As each unit cell contains sixteen chains and eight crosslinks, our rigid elastomers contain up to 73728 LC molecules and 4096 crosslinking sites (for a total of 77824 particles), corresponding to a crosslinker density of 5.26%. Periodic boundaries are used to mimic bulk conditions. The role of defects in the network topology is considered in the Supplementary Information (SI) [28].

Mesogens interact through a Gay–Berne (GB) potential energy function [24, 25], with parameter values matching those employed by Gay and Berne in their original work [24]. The ellipsoidal aspect ratio is 3, while the ratio of potential well depths for side-to-side and end-to-end interactions is 5. The dimensionless parameters μ and ν are set to 2 and 1, respectively. The van der Waals diameter (σ_0) interaction strength (ε_0), and mass (m) of mesogens are set to unity. This model is used frequently to describe LC systems [29], and its phase behavior has been reported in the literature [30]. Expanded finitely extensible nonlinear elastic (FENE) bonds [31] are employed for polymer chains, connecting neighboring mesogen centers-of-mass. Backbone bonds having equilibrium bond length $l_b = 2\sigma_0$ and maximum deviation $R = 2\sigma_0$ and strength $10\varepsilon_0$, while cross-linker–chain bonds having corresponding parameters for strength $1000\varepsilon_0$, $l_b = \sigma_0$ and $R = 3\sigma_0$. These parameters are chosen to maximize orientational pinning effects due to crosslinking particles and promote formation of a polydomain state while accelerating the relaxation of chain-bound mesogens. Simulations are performed at constant temperature $T^* = k_B T / \varepsilon_0 = 0.7$ (where starred quantities henceforth denote Lennard-Jones reduced units [32]) using a Langevin thermostat with pressure controlled via a Nosé-Hoover barostat. In the absence of an elastic network, the state point (P^*, T^*) considered in this work results in a smectic-B phase. Though monodomain smectics have different soft-elastic properties than nematics [33], the mechanical response during the P–M transition is expected to be unaffected [9]. Details of our sample preparation procedure are included in the SI [28].

Orientationally ordered mesogen phases are distinguished via the scalar order parameter S, which represents the maximum positive eigenvalue of the Q-tensor

$$Q_{\alpha\beta} = \frac{1}{2N} \sum_{i=1}^{N} [3u_{i\alpha} u_{i\beta} - \delta_{\alpha\beta}] \ . \tag{2}$$

Here $u_{i\alpha}$ is the α component of the orientation u_i of particle i, N is the number of particles, and $\delta_{\alpha\beta}$ is the Kronecker-delta. The corresponding eigenvector $\hat{\mathbf{n}}$ defines domain orientation. Systems with a global value $S \approx 0$ are considered isotropic; systems with $S > 0.3$ are distinguished as nematic or smectic depending on the degree of positional order.
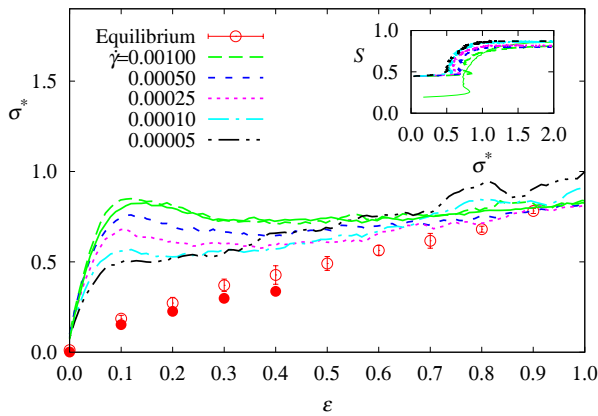
FIG. 2. (Color Online) Stress–strain behavior. Upon the application of strain, an initial elastic regime is observed for constant-strain-rate deformations. The strain rate $\dot{\gamma}$ is given in units of $1/t^*$. After an initial stress overshoot, the system relaxes back to a characteristic plateau, where the stress increases only weakly as a function of strain. Dashed curves are for an $N = 9728$ system, while the solid green curve is for an $N = 77824$ system at strain rate $\dot{\gamma} = 10^{-3}$. Red symbols show the equilibrium behavior for $N = 9728$ (open circles) and $N = 77824$ (solid circles) systems. Inset: The nematic order parameter increases sharply upon reaching a characteristic stress, which is weakly dependent on strain rate.

To elucidate the molecular mechanism underlying the P–M transition, we must characterize randomly oriented nematic domains in the system. This is done by identifying and merging particle clusters. Initial domains are defined as the largest spherical regions centered at a particle with nematic order parameter greater than a value S_c. If two spherical domains overlap and have a combined order parameter higher than S_c, they are merged into a single domain. We use $S_c = 0.6$ to ensure constituent particles have roughly the same orientation across the merged domain. Particles in the overlap region of two domains are assigned to their best fit (according to the value of $\hat{\mathbf{u}}_i \cdot \hat{\mathbf{n}}$) if the domains are not merged.

Fig. 1a shows a representative configuration of an equilibrium LCE with rigid crosslinkers in the absence of external stress. Particles are colored according to their local molecular orientation. One can observe distinct domains comprising several hundreds to thousands of particles that assume different orientations; the system is in a polydomain state. It should be noted that despite the polydomain structure, a scalar order parameter $S > 0.3$ is observed in many runs due to the existence of large domains (compared to the simulation box). As a uniaxial strain is applied, clusters reorient and merge (cf Fig. 1b). The result is a dominant large cluster interdispersed with a few smaller domains. Above a threshold strain value, a single monodomain state is observed (cf Fig. 1c). Within these images, some positional ordering of the mesogens can be observed—to characterize that ordering, we compute the radial distribution function for particles within the system (cf Fig. 3c). A distinct set of coordination layers is evident around each mesogen, suggestive of local smectic ordering at zero strain.

The mechanical response of the system is depicted in Fig. 2, with stress plotted as a function of strain for five different strain rates. Each of these is averaged over five independent realizations of the LCE system for sizes $N = 9728$ (dashed lines) and $N = 77824$ (solid line). After an initial elastic regime [28], these exhibit a stress overshoot, commonly observed in experiments on LCEs [1], which relaxes to a plateau that is apparently independent of strain rate. Comparison to an equilibrium curve (red circles—9728 [open] and 77824 [solid]), obtained by allowing the stress to relax to a constant value (determined by block averaging) for different step-strains, indicates the response of the model elastomers proposed here is analogous to that of the side-chain LCEs in Ref. [15], where the threshold yield stress decreases with strain rate. Such side-chain LCEs do not exhibit an equilibrium plateau stress. Indeed, we observe exactly this, as the stress–strain response is monotonic, and almost linear for $\varepsilon \in [0.1, 0.9]$; beyond that strain the equilibrium curve merges with those obtained at constant strain rate. The inset of Fig. 2 shows the order parameter as a function of strain. The initial polydomain state exhibits a steep jump in order parameter as a threshold stress is crossed. The value of this stress is only weakly dependent on the strain rate over the range considered here. Further, this threshold stress $\sigma^* \approx 0.5$ corresponds to the onset of a linear restoring force after the soft-elastic region. This is consistent with the theoretical prediction of Ref. [14], where a sharp increase in orientational ordering was predicted upon the advent of the P–M transition.

Fig. 3a shows the distribution of domain sizes in equilibrium as a function of step strain. At equilibrium, most particles form clusters of 100–1000 particles. This distribution is strongly altered by the application of a step strain, with small domains disappearing as clusters merge to form larger domains. Fig. 3b shows the distribution of domain orientations relative to the axis of extension. We observe that, at equilibrium, domains are oriented randomly. Upon application of strain, however, these reorient in a manner that better accommodates the local strain. As a result, domains begin aligning with the stretching direction, evidenced by the enhancement in probability for small θ. Taken together, these observations suggest the P–M transition of SCLCEs proceeds through a combination of domain rotation and subsequent growth, rather than the pure domain reorientation mechanism proposed from experiments on main-chain LCEs [18]. Note that spatial structure is largely unchanged by strain. Fig. 3c shows the radial distribution of mesogens (of both chain and crosslink varieties) varies only near contact, with contact probability decreasing for chain mesogens and marginally increasing for crosslinks.
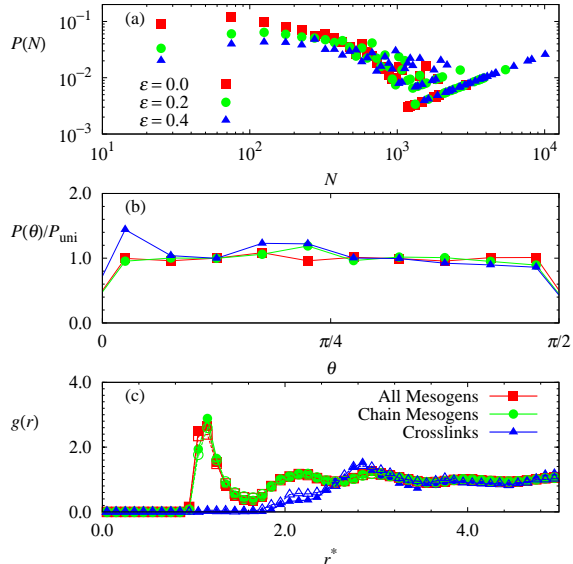
FIG. 3. (Color Online) Equilibrium structures within large ($N = 77824$) model LCEs. (a) Probability of finding a mesogen in a cluster of size N after equilibration at different step strains, averaged over five independent realizations of the system. Initially, most particles are in clusters of size 10^2–10^3. Clusters merge as the strain is increased, shifting the size distribution. Eventually, all particles are observed to be part of a single cluster with $S \geq 0.6$. (b) Orientation distribution of nematic domains, normalized by an isotropic distribution ($P(\theta) \propto \sin\theta$). Nematic directors rotate as step strains are applied, and align with the direction of strain ($\theta = 0$). (c) Radial distribution function for mesogens within the system. Layering, indicative of smectic ordering, is observed between mesogens attached to the polymer backbone. Liquid-like, isotropic correlations are observed between crosslinker particles. Solid lines (connecting solid symbols) show the mesogen distribution under equilibrium conditions, while dashed lines (connecting open symbols) show the mesogen distribution after uniaxial strain at $\dot{\gamma} = 0.001$ to $\varepsilon = 5$. The spatial distribution of particles is largely unaffected.

The dynamics of individual clusters within a sample are examined as a function of time at constant strain rate $\dot{\gamma} = 10^{-3}t^{*-1}$. Fig. 4 shows the evolution of several domains. For clarity, only 3 domains are shown: one with a director parallel to the strain direction ($\hat{\mathbf{x}}$), one with a director perpendicular to $\hat{\mathbf{x}}$, and a third corresponding to the largest domain in the system. We observe fluctuations in the individual domain sizes as the simulation progresses, with most particles aggregating into a single large cluster after $1000t^*$ ($\varepsilon = 2.0$). Interestingly, each domain begins with a high degree of local order, $S \geq 0.8$, which decays as misaligned particles become incorporated. Further, large domains which are nearly perpendicular to the nematic director persist until $\varepsilon \approx 0.15$, which coincides with the onset of soft elasticity (or the stress plateau), after which point they gradually rotate and merge with the
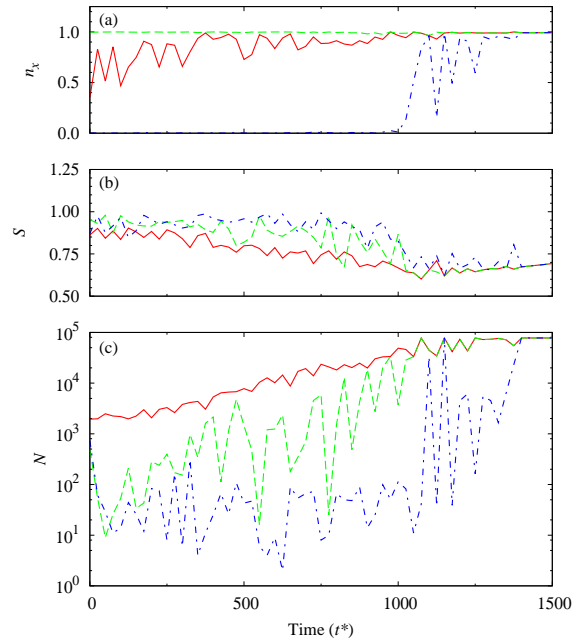

FIG. 4. (Color Online) Domain dynamics at constant strain rate for a representative system. Depicted are the largest cluster (solid red line), the cluster best aligned with the direction of strain (dashed green line) and the cluster most perpendicular to the direction of strain (dash-dotted blue line). (a) The component of the nematic director along the strain axis. (b) The order parameter of each cluster. (c) The size of each cluster. The strain rate is $\dot{\gamma} = 10^{-3}t^{*-1}$.

largest domain. This result further validates our conclusion that the P–M transition in our model system occurs via domain reorientation and growth.

In conclusion, a coarse-grained molecular model of LC elastomers has been proposed and has been shown to reproduce the experimentally observed soft elasticity behavior, upon which a small applied stress can lead to a large deformation. The observed soft elasticity is shown to correspond to a polydomain-to-monodomain transition of the LCE material, and is accompanied by a sudden increase of the nematic scalar order parameter. Our model and simulations are the first to reproducibly produce well-defined polydomain states at zero stress and, more importantly, provide direct evidence that when stress is applied to a polydomain material, the domains rotate and merge, thereby leading to a stress plateau and a macroscopic deformation. Past experimental reports [16] had proposed that domain rotation is responsible for the stress plateau in LCEs; our computational results support such a view and indicate that nucleation of large domains from the initial polydomain state is also an important mechanism in the transition. While the results presented here have been generated on the basis of a simple coarse grained model, they serve to provide a first molecular-level demonstration of a polydomain–

monodomain transition, and offer a starting point for the investigation of the influence of molecular details on the stress response of LCEs.

---

* depablo@uchicago.edu

[1] M. Warner and E. M. Terentjev, *Liquid Crystal Elastomers* (Oxford University Press, New York, 2003).

[2] A. R. Tajbakhsh and E. M. Terentjev, Eur. Phys. J. E **6**, 181 (2001).

[3] H. Finkelmann, A. Greve, and M. Warner, Eur. Phys. J. E **5**, 281 (2001).

[4] J. V. Selinger, H. G. Jeon, and B. R. Ratna, Phys. Rev. Lett. **89**, 225701 (2002).

[5] J. Naciri, A. Srinivasan, H. Jeon, N. Nikolov, P. Keller, and B. R. Ratna, Macromolecules **36**, 8499 (2003); D. Corbett and M. Warner, Sens. Actuators A **149**, 120 (2009); Y. Y. Huang, J. Biggins, Y. Ji, and E. M. Terentjev, J. Appl. Phys. **107**, 083515 (2010).

[6] D. L. Thomsen, P. Keller, J. Naciri, R. Pink, H. Jeon, D. Shenoy, and B. R. Ratna, Macromolecules **34**, 5868 (2001); D. K. Shenoy, D. L. Thomsen, A. Srinivasan, P. Keller, and B. R. Ratna, Sens. Actuators A **96**, 184 (2002).

[7] P. A. Bermel and M. Warner, Phys. Rev. E **65**, 056614 (2002); T. Hiscock, M. Warner, and P. Palffy-Muhoray, J. Appl. Phys. **109**, 104506 (2011).

[8] H. Finkelmann, H. J. Kock, and G. Rehage, Makromol. Chem. Rapid Commun. **2**, 317 (1981).

[9] C. Ortiz, M. Wagner, N. Bhargava, C. K. Ober, and E. J. Kramer, Macromolecules **31**, 8531 (1998); A. Sánchez-Ferrer and H. Finkelmann, Macromol. Rap. Comm. **32**, 309 (2011).

[10] J. Schatzle, W. Kaufhold, and H. Finkelmann, Macromol. Chem. Phys. **190**, 3269 (1989).

[11] J. Kupfer and H. Finkelmann, Macromol. Chem. Phys. **195**, 1353 (1994).

[12] M. Warner, P. Bladon, and E. M. Terentjev, J. Phys. II **4**, 93 (1994), journal de Physique, France.

[13] P. D. Olmsted, J. Phys. II **4**, 2215 (1994), journal de Physique, France.

[14] S. V. Fridrikh and E. M. Terentjev, Phys. Rev. E **60**, 1847 (1999).

[15] A. Hotta and E. M. Terentjev, J. Phys.: Condens. Matter **13**, 11435 (2001).

[16] S. M. Clarke, E. Nishikawa, H. Finkelmann, and E. M. Terentjev, Macromol. Chem. Phys. **198**, 3485 (1997).

[17] S. V. Fridrikh and E. M. Terentjev, Phys. Rev. Lett. **79**, 4661 (1997).

[18] S. M. Clarke, E. M. Terentjev, I. Kundler, and H. Finkelmann, Macromolecules **31**, 4862 (1998).

[19] D. B. Liarte, S. R. Salinas, and C. S. O. Yokoi, Phys. Rev. E **84**, 011124 (2011).

[20] G. Skačej and C. Zannoni, Eur. Phys. J. E **25**, 181 (2008).

[21] P. Pasini, G. Skačej, and C. Zannoni, Chem. Phys. Lett. **413**, 463 (2005).

[22] G. Skačej and C. Zannoni, Soft Matt. **7**, 9983 (2011); Proc. Natl. Acad. Sci. U.S.A. **109**, 10193 (2012).

[23] A. A. Darinskii, A. Zarembo, N. K. Balabaev, I. M. Neelov, and F. Sundholm, Macromol. Symp. **237**, 119 (2006); A. A. Darinskii, A. Zarembo, and N. K. Balabaev, **252**, 101 (2007).

[24] J. G. Gay and B. J. Berne, J. Chem. Phys. **74**, 3316 (1981).

[25] D. J. Cleaver, C. M. Care, M. P. Allen, and M. P. Neal, Phys. Rev. E **54**, 559 (1996).

[26] M. Bispo, D. Guillon, B. Donnio, and H. Finkelmann, Macromolecules **41**, 3098 (2008).

[27] F. A. Escobedo and J. J. dePablo, J. Chem. Phys. **104**, 4788 (1996).

[28] See Supplemental Material at [**URL**] for further information about the equilibration routine, elastic stress-strain response, and the effect of defects in the elastic network topology.

[29] M. Wilson, Int. Rev. Phys. Chem. **24**, 421 (2005).

[30] E. de Miguel, L. F. Rull, M. Chalam, and K. E. Gubbins, Mol. Phys. **71**, 1223 (1990); E. de Miguel, L. F. Rull, M. K. Chalam, and K. E. Gubbins, **74**, 405 (1991); E. de Miguel, L. F. Rull, M. K. Chalam, K. E. Gubbins, and F. van Swol, **72**, 593 (1991); E. de Miguel, L. F. Rull, and K. E. Gubbins, Phys. Rev. A **45**, 3813 (1992); J. T. Brown, M. P. Allen, E. Martín del Río, and E. de Miguel, Phys. Rev. E **57**, 6685 (1998); M. Bates and G. Luckhurst, in *Liquid Crystals I*, Structure and Bonding, Vol. 94, edited by M. P. Mingos (Springer, 1999) Chap. 3, pp. 65–137.

[31] K. Kremer and G. S. Grest, J. Chem. Phys. **92**, 5057 (1990).

[32] M. P. Allen and D. J. Tildesley, *Computer Simulation of Liquids* (Clarendon, Oxford, 1987).

[33] J. M. Adams and M. Warner, Phys. Rev. E **71**, 021708 (2005); **72**, 011703 (2005).